

Nanoscale

Accepted Manuscript



This is an *Accepted Manuscript*, which has been through the Royal Society of Chemistry peer review process and has been accepted for publication.

Accepted Manuscripts are published online shortly after acceptance, before technical editing, formatting and proof reading. Using this free service, authors can make their results available to the community, in citable form, before we publish the edited article. We will replace this *Accepted Manuscript* with the edited and formatted *Advance Article* as soon as it is available.

You can find more information about *Accepted Manuscripts* in the [Information for Authors](#).

Please note that technical editing may introduce minor changes to the text and/or graphics, which may alter content. The journal's standard [Terms & Conditions](#) and the [Ethical guidelines](#) still apply. In no event shall the Royal Society of Chemistry be held responsible for any errors or omissions in this *Accepted Manuscript* or any consequences arising from the use of any information it contains.

Cite this: DOI: 10.1039/c0xx00000x

www.rsc.org/xxxxxx

COMMUNICATION**High-yield synthesis of triangular gold nanoplates with improved shape uniformity, tunable edge length and thickness**

Youju Huang, Abdul Rahim Ferhan, Yi Gao, Anirban Dandapat and Dong-Hwan Kim*

Received (in XXX, XXX) Xth XXXXXXXXX 20XX, Accepted Xth XXXXXXXXX 20XX

DOI: 10.1039/b000000x

We report the synthesis of uniform triangular gold nanoplates by a modified seeded growth method. The concentration of cetyltrimethylammonium bromide (CTAB) in the growth solution and the time interval between multiple steps of growth were important factors which determine the formation of uniform triangular Au nanoplates. In addition, by further isotropic overgrowth, the thickness of triangular Au nanoplates can be finely tuned within a wide range of 10–80 nm, which at present remains a challenge using conventional seeded growth.

It has been well established that the size,^{1–3} shape^{4–7} and composition^{8–10} of noble metal nanoparticles (NPs) can significantly affect their physical and chemical properties. Noble metal NPs have vast potential for numerous practical applications such as selective catalysis,^{11, 12} information storage,¹³ nanomedicine,^{14, 15} biosensors,^{16–20} photothermal heating²¹ and enhanced imaging.²² Among various noble metal nanomaterials, anisotropic gold NPs are particularly interesting because of their decreased geometrical symmetry which induces new and distinctive properties.²³ Anisotropic gold nanorods (AuNRs) exhibiting transverse and longitudinal resonances represent a fine example, whereby the tunability of their longitudinal surface plasmon wavelengths (LSPWs) makes them favorable for many practical applications such as photonic devices,¹³ orientation sensors,²⁴ medical diagnostics and therapeutics.^{25, 26}

In contrast to the mature synthetic technique^{27–33} and extensive applications of AuNRs,^{15, 34} there is surprisingly not much attention on another very important member of the anisotropic family of AuNPs- i.e. Au nanoplates. Similar to AuNRs, triangular Au nanoplates have also two surface plasmon absorption bands including a strong absorption band in the near-infrared (NIR) region, making them highly suitable for biological applications. Because the energy from NIR is much lower than those from visible and ultraviolet regions, operating in NIR will avoid or significantly reduce potential damages to biological tissues and cells. Furthermore, light in this region can maximally penetrate biological tissues due to the minimal optical absorption by hemoglobin and water.^{35, 36} More importantly, unlike AuNPs of other shapes, triangular Au nanoplates can easily provide plasmonic responses in the wavelength region of 1000 to 1400 nm, which is the second *in vivo* bioimaging window.³⁷ Apart from biological significance, it was also reported that triangular

Au nanoplates could show anisotropic electrical conductivity,³⁸ strong enhancement of electric field³⁹ and enhanced catalytic properties⁴⁰ compared with isotropic AuNPs.

While the potential applications are numerous, it is often difficult to prepare uniform triangular Au nanoplates in high yield. The synthesis of triangular Au nanoplates have been achieved via various routes, such as thermal methods,⁴¹ seeding,⁴² photocatalytic⁴³ and biological approaches.³⁹ However the resulting solution contains relatively high percentage of AuNPs of other shapes, such as spheres and rods. For example, Sastry and co-workers³⁹ prepared triangular Au plates in an edge size range from 0.05 to 1.8 μm using biological synthesis, and approximately 50% of Au nanospheres were found in the final product. Mirkin and co-workers⁴² prepared triangular Au plates with the average edge length of 144 nm by seed-mediated growth, which also resulted in approximately 50% of spherical AuNPs, hence requiring a purification process. Another very important issue in the synthesis of triangular Au nanoplates is related to the tuning of their thickness, which significantly alter the degree of anisotropy to tune their plasmonic properties.²³ However, while there are many studies which investigated the edge length tunability, there are rare reports on tuning the thickness of triangular Au nanoplates.

It has been proposed that surfactants (e.g., cetyltrimethylammonium bromide (CTAB) and polyvinylpyrrolidone (PVP)), play a key role in the asymmetric growth of NPs leading to nanotriangles.⁴³ Small changes in surfactant concentration could lead to large changes in the morphology of the resulting NPs.⁴⁴ Recently, Xia and co-workers found that precise control over the kinetic reactions,^{45–47} especially, reaction rate controlled by the time and sequence of added reagents, also significantly affect the morphology and uniformity of the final metal NPs. Herein we describe a modified, seed-mediated growth method for the high yield synthesis of uniform triangular Au nanoplates using an optimized CTAB growth solution and appropriate time interval between multiple growth steps. The obtained triangular Au nanoplates can be three dimensionally enlarged by further isotropic overgrowth. As a result, different edge length and thickness of triangular Au nanoplates are obtained, which ultimately results in a broadly tunable surface plasmon resonance from 800 to 1346 nm in the NIR region.

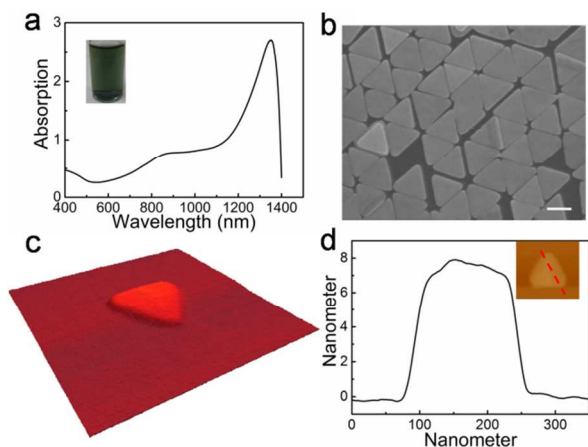


Fig. 1 UV-vis-NIR absorption spectrum (a), digital photograph (insert image), and representative SEM images of triangular Au nanoplates obtained at optimized conditions (3 s time interval and 0.025 M of CTAB); 3D tapping mode AFM image (c) of single triangular Au nanoplate and its corresponding height profile (d). The scan size for 3D AFM image (c) is 500 nm². The scale bar in b represents 100 nm.

Digital photograph and UV-vis-NIR absorption spectrum of the sample obtained at optimized conditions are shown in Fig. 1a. Two absorption peaks at 709 nm and 1300 nm in the spectrum corresponding to the in-plate dipole and quadrupole plasmon resonances of our triangle Au nanoplates.⁴⁸ It is worth noting that the peak at 1300 nm is relatively stronger than those in the previous report,^{43, 49} and no peak is observed at 500–600 nm, indicating an exceptionally high purity of triangle Au nanoplates with very few spherical AuNPs in the suspension. The SEM image Fig. 1b confirmed the high uniformity of the obtained triangle nanoplates, with few byproducts. The average edge length of synthesized triangle Au nanoplates is 140 nm, and the monodispersity in edge length is significantly improved (relative standard deviation (RSD) of ~5.1%) compared with those in previous reports.^{39, 42} Atomic force microscope (AFM) image of the triangle Au nanoplates confirms that their lateral surfaces are atomically flat with a uniform thickness of 8.0±0.5 nm.

The effects of the CTAB concentration and time interval between continuous growth steps on the uniformity and purity were systematically studied. Fig. 2 shows SEM images of Au plates obtained using different concentrations of CTAB in growth solution and a constant time interval between continuous growth steps (i.e., 5 s). At low concentration of CTAB (0.01 M), the Au seeds grow into both plate and non-plate shaped NPs. The amount of Au plates obtained using a low CTAB concentration was estimated to be ca. 40%. As a result, the corresponding UV-vis-NIR spectra (Fig. 3A-4) shows a strong peak at approximately 540 nm corresponding to spherical shapes, in addition to the absorption peaks at 650 nm and 1200 nm ascribed to Au plates. At a CTAB concentration of 0.025 M, the seeds favor the growth into triangular Au plates in high yield (Fig. 2b), exhibiting strong and sharp absorption peaks at around 800 nm and 1300 nm resulting from Au plates (Fig. 3a-3). Non-plate shaped byproducts were hardly found, leading to the disappearance of the 540 nm peak corresponding to spherical shapes.¹ However, at much higher concentrations of CTAB (0.05 M and 0.1), hexagonal, circular and truncated triangular Au plates appeared, resulting in the broader and weaker plasmonic peaks

(Fig. 3a-1 and a-2) than that from 0.025 M of CTAB.

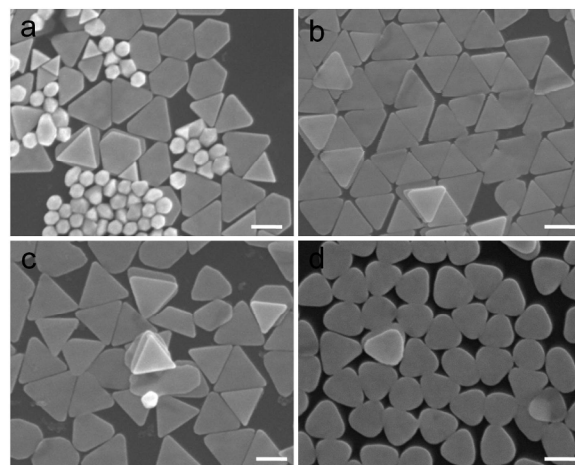


Fig. 2 Representative SEM images of triangular Au nanoplates obtained at different concentrations of CTAB in growth solution (a: 0.01 M; b: 0.025 M; c: 0.05 M; d: 0.1 M). The scale bars represent 100 nm.

This indicates that a fine balance of a CTAB concentration is required to attain a high yield of uniform triangle Au nanoplates. It is widely accepted that a high concentration of CTAB can block some facets of seeds and lead to a two dimensional deposition of Au atoms,^{23, 42} further favouring the formation of triangle Au nanoplates. This can be confirmed by the thickness of triangle Au nanoplates (8 nm, Fig. 1d), which is close to the average diameter of the seed when the two layers of CTAB on the two sides of triangle Au nanoplates were included. However, excess free CTAB in solution have the detrimental influences on the deposition of Au atoms on the seed surface. Firstly, the exchange balance between the surface CTAB on seeds and gold atoms becomes out of balance by the excess free CTAB in solution. Secondly, the excess CTAB molecules interacting with gold ions in solution may form small nanoparticles by self-nucleation process. Both of which often results in compromised uniformity of resultant nanoparticles.

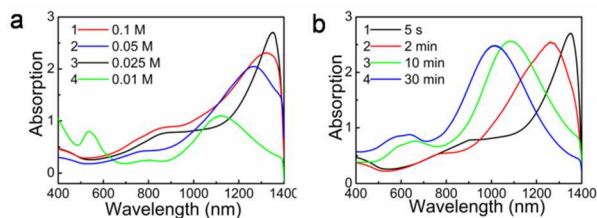


Fig. 3 UV-vis-NIR absorption spectrum of triangular Au nanoplates obtained at different concentrations of CTAB in growth solution (a) and different time intervals (b) between multiple growth steps.

Compared to single step growth, a big advantage of multiple step growth lies in its ability to efficiently avoid secondary nucleation.^{50, 51} Shortening the time interval between multiple step growths is expected to maximally decrease the probability of secondary homogenous nucleation. In our present study, we found that a short time interval can not only dramatically improve the uniformity, but also can finely tune the size of resultant triangle Au nanoplates. Figure 4a-d shows SEM images of

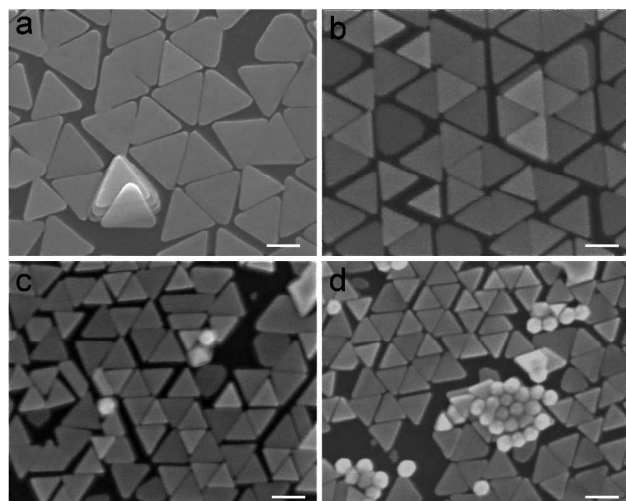


Fig. 4 Representative SEM images of triangular Au nanoplates obtained at different time intervals between multiple growth steps (a: 5 s; b: 2 min; c: 10 min; d: 30 min). The scale bars represent 100 nm.

triangle Au nanoplates obtained at the time interval of 5 s, 2, 10, and 30 min, respectively. It can be clearly observed that the edge length of triangle Au nanoplates (Fig. 4a) at short time interval (5 s) is in high monodispersity. As the time interval increases, smaller triangle Au nanoplates (edge length around 80 nm) begin to appear (Fig. 4b), leading to a blue-shift and peak broadening of the quadrupole plasmon resonance (Fig. 3b). Longer time intervals (10 min and 30 min) resulted in a majority of smaller triangle Au nanoplates, accompanied by spherical NPs (Fig. 4c and d). The appearance of relatively small NPs significantly affected their corresponding plasmon resonances; the quadrupole plasmon resonances of triangle Au nanoplates at time intervals of

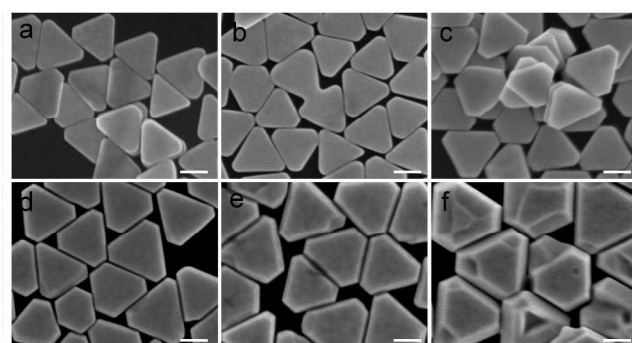


Fig. 5 Representative SEM images of triangular Au nanoplates by further isotropic overgrowth (the volume amount ratio between isotropic growth solution and triangular Au nanoplates (sample in Fig. 1b) in a-f are 2, 6, 10, 20, 40 and 100, respectively). The scale bars represent 100 nm.

10 min and 30 min shifted to 1082 and 1010 nm, respectively, and a peak shoulder at around 550 nm appeared due to the presence of spherical NPs.

An effective and powerful way to tailor the size of NPs, while keeping their initial shape, is to control the isotropic growth of initial seeds. In our previous work,^{1, 2} we have used optimized CTAB growth solution to isotropically grow Au spherical and rod-shaped seeds into bigger and size-tuneable spheres and rods,

respectively. The isotropic growth solution contains a lower concentration of CTAB (0.01 M) than that of the standard growth solution (0.1 M).²⁷ This approach would offer the same growth rate in all directions from the seed and significantly decrease the possibility of secondary homogeneous nucleation, enabling controlled enlargement of Au seeds, while avoiding the formation of other shaped NPs. Fig. 5 shows the evolution of triangle Au nanoplate (the sample from Fig. 1b) seeds with gradual increase in the amount of growth solution. It is obvious that the edge length of triangle Au nanoplates increases with increasing volume amount ratio between isotropic growth solution and triangular Au nanoplates. The original triangular Au nanoplates (Fig. 1b) have an average edge length of 140 nm. During the isotropic growth, the edge length increases to 147, 158, 186, 204, 216 and 257 nm corresponding to the amount ratio of 2, 6, 10, 20, 40 and 100, respectively. The edge length change is not exactly proportional to amount of growth solution. Triangular Au nanoplates tend to lose their angular corners (Fig. 5c-f) when the amount ratio is larger than 10. It is also clear to see bumps and cavities (Fig. 5e and f) on the surfaces of the truncated triangle Au nanoplates, which implies the increase of the nanoplate thickness.

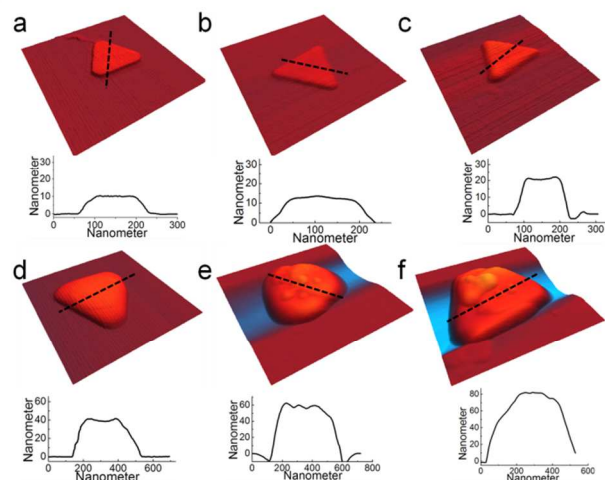


Fig. 6 Representative 3D tapping mode AFM images (a-f) and their corresponding height profile (the thicknesses in a-f are 10, 13, 20, 40, 60 and 83 nm, respectively) of triangular Au nanoplates by further isotropic overgrowth (the volume amount ratio between isotropic growth solution and triangular Au nanoplates (sample in Fig. 1b) in a-f are 2, 6, 10, 20, 40 and 100, respectively). The scan size for 3D AFM images (a-f) is 500 nm².

The thickness of nanoplates was systematically investigated by AFM. Fig. 6 shows 3D tapping mode AFM images of enlarged triangular Au nanoplates (Fig. 6a-f) and their corresponding height profiles (Fig. 6a'-f'). The 3D tapping mode images further confirm the surface changes from a flat to a bumpy morphology. The height profiles clearly display the thickness of triangular Au nanoplates. The thickness can be finely tuned within a wide range from 10 to 83 nm by simply varying the amount of growth solution. To the best of our knowledge, this is the first report which demonstrates the tailoring of triangular Au nanoplates thickness within such a wide range.

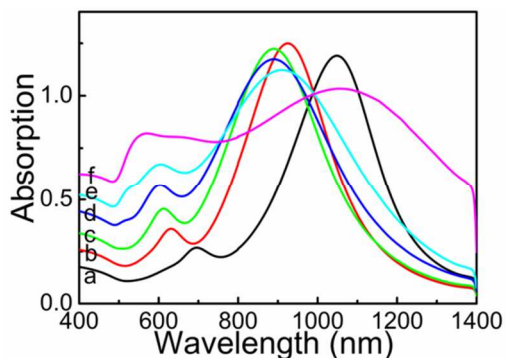


Fig. 7. UV-vis-NIR absorption spectrum of triangular Au nanoplates by further isotropic overgrowth (the volume amount ratio between isotropic growth solution and triangular Au nanoplates (sample in Fig. 1b) in a-f are 2, 6, 10, 20, 40 and 100, respectively).

The ability to tailor the thickness and edge length of triangular Au nanoplates within a broad dimensional window leads to the tunability of surface plasmon resonance wavelength in a wide range. Fig. 7 shows UV-vis-NIR absorption spectrum of triangular Au nanoplates with edge lengths and thickness. The first plasmonic peak (in shorter wavelength range), attributed to the in-plate dipole plasmon resonance, was initially observed at 709 nm (Fig. 1a). This peak gradually blue-shifted to 561 nm with an increasing amount of growth solution. The second peak (in longer wavelength range), attributed to the quadrupole plasmon resonance was initially positioned at 1300 nm (Fig. 1a). This peak first blue-shifted and then red-shifted to a final position at around 1080 nm. The turning point occurs at an amount ratio of 20 between isotropic growth solution and triangular Au nanoplate seeds, where the peak wavelength is 893 nm. Theoretical studies⁴⁸ have shown that the in-plate dipole plasmon resonance is dominated by charge accumulation at corners. As the amount of the isotropic growth solution increases, the tips of the nanoplates change from being sharp to truncated, which possibly resulted in the blue-shift of the in-plate dipole plasmonic peak. On the other hand, the quadrupolar plasmonic peak is directly related to charge accumulation along the sides and the corners of triangular Au nanoplate, which can be thought as the resonance in the longitudinal direction. It is dependent on the aspect ratio between the edge length and thickness. As the isotropic growth solution is increased, both the edge length and thickness of triangular Au nanoplates would increase. This would lead to the decrease of aspect ratio, inducing a blue-shift of plasmonic peak wavelength. However, as the thickness is increased, the surface morphology of triangular Au nanoplates also changed. The appearance of bumps and cavities would lead to a discontinuous surface and significantly affects the plasmon resonance. Similar to plasmonic percolation behaviours,⁵² the plasmonic peak would red-shift.

We have demonstrated that by fine control over experimental parameters such as the concentration of CTAB in growth solution and the time interval between multiple steps of growth, triangle Au nanoplates with simultaneously improved purity and edge length uniformity compared to conventional seeded growth methods can be synthesized by reducing the concentration of CTAB (as low as 0.025 M). Not only thin triangle Au nanoplates (thickness around 8 nm) with broadly tunable surface plasmon

resonances in NIR can be made, but more importantly, thick triangle Au nanoplates with thickness tunable up to 80 nm can be synthesized using further isotropic overgrowth. Tailored synthesis of triangular Au nanoplates with simultaneous improvements in uniformity and yield will not only help to better understand the mechanism of seed-mediated growth of triangular Au nanoplates but also advance the research on anisotropic plasmonic nanomaterials.

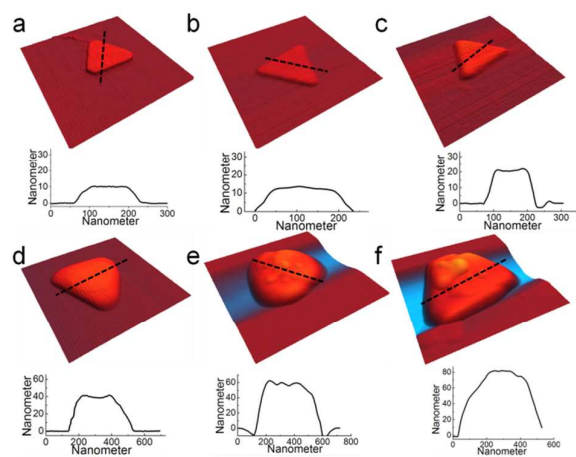
Acknowledgements

We gratefully acknowledge the financial support of the Ministry of Education of Singapore (MOE2012-T2-1-058).

References

- School of Chemical and Biomedical Engineering, Nanyang Technological University, 637457, Singapore*
 Fax: 65 6791 1761; Tel: 65 6315 8825; E-mail: dhkim@ntu.edu.sg
- † Electronic Supplementary Information (ESI) available: [details of Experimental procedure]. See DOI: 10.1039/b000000x/
1. Y. Huang and D. H. Kim, *Langmuir*, 2011, **27**, 13861-13867.
 2. Y. Huang and D. H. Kim, *Nanoscale*, 2011, **3**, 3228-3232.
 3. L. Hwang, G. Zhao, P. Zhang and N. L. Rosi, *Small*, 2011, **7**, 1939-1942.
 4. M. H. Huang and P. H. Lin, *Adv. Funct. Mater.*, 2012, **22**, 14-24.
 5. Y. Huang and D. H. Kim, *Nanoscale*, 2012, **4**, 6312-6317.
 6. Y. Huang, L. Wu, X. Chen, P. Bai and D. H. Kim, *Chem. Mater.*, 2013, **25** 2470-2475.
 7. H. G. Liao, Y. X. Jiang, Z. Y. Zhou, S. P. Chen and S. G. Sun, *Angew. Chem. Int. Ed.*, 2008, **47**, 9100-9103.
 8. E. Ringe, J. M. McMahon, K. Sohn, C. Cobley, Y. Xia, J. Huang, G. C. Schatz, L. D. Marks and R. P. Van Duyne, *J. Phys. Chem. C*, 2010, **114**, 12511-12516.
 9. P. K. Jain, X. Huang, I. H. El-Sayed and M. A. El-Sayed, *Acc. Chem. Res.*, 2008, **41**, 1578-1586.
 10. Y. Huang, A. R. Ferhan and D.-H. Kim, *Nanoscale*, 2013, **5**, 7772-7775.
 11. S. Navalon, R. Martin, M. Alvaro and H. Garcia, *Angew. Chem., Int. Ed.*, 2010, **49**, 8403-8407.
 12. A. M. Chen, O. Taratula, D. Wei, H. I. Yen, T. Thomas, T. J. Thomas, T. Minko and H. He, *ACS Nano*, 2010, **4**, 3679-3688.
 13. P. Zijlstra, J. W. M. Chon and M. Gu, *Nature*, 2009, **459**, 410-413.
 14. E. Boisselier and D. Astruc, *Chem. Soc. Rev.*, 2009, **38**, 1759-1782.
 15. X. Huang, S. Neretina and M. A. El-Sayed, *Adv. Mater.*, 2009, **21**, 4880-4910.
 16. L. Guo, A. R. Ferhan, H. Chen, C. Li, G. Chen, S. Hong and D. H. Kim, *Small*, 2013, **9**, 234-240.
 17. L. Guo, Y. Huang, Y. Kikutani, Y. Tanaka, T. Kitamori and D. H. Kim, *Lab Chip*, 2011, **11**, 3299-3304.
 18. L. Guo, Y. Xu, A. R. Ferhan, G. Chen and D.-H. Kim, *J. Am. Chem. Soc.*, 2013, **135**, 12338-12345.
 19. L. Guo, X. Zhou and D. H. Kim, *Biosens. Bioelectron.*, 2011, **26**, 2246-2251.
 20. B. Wu, L.-C. Chen, Y. Huang, Y. Zhang, Y. Kang and D.-H. Kim, *Plasmonics*, 2014, 1-7.

21. P. M. Bendix, S. N. S. Reihani and L. B. Oddershede, *ACS Nano*, 2010, **4**, 2256-2262.
22. J. Ando, K. Fujita, N. I. Smith and S. Kawata, *Nano Lett.*, 2011, **11**, 5344-5348.
23. J. E. Millstone, S. J. Hurst, G. S. Métraux, J. I. Cutler and C. A. Mirkin, *Small*, 2009, **5**, 646-664.
24. W. S. Chang, J. W. Ha, L. S. Slaughter and S. Link, *Proc. Natl. Acad. Sci. U. S. A.*, 2010, **107**, 2781-2786.
25. X. Huang, I. H. El-Sayed, W. Qian and M. A. El-Sayed, *J. Am. Chem. Soc.*, 2006, **128**, 2115-2120.
26. C. C. Chen, Y. P. Lin, C. W. Wang, H. C. Tzeng, C. H. Wu, Y. C. Chen, C. P. Chen, L. C. Chen and Y. C. Wu, *J. Am. Chem. Soc.*, 2006, **128**, 3709-3715.
27. B. Nikoobakht and M. A. El-Sayed, *Chem. Mater.*, 2003, **15**, 1957-1962.
28. W. Ni, X. Kou, Z. Yang and J. Wang, *ACS Nano*, 2008, **2**, 677-686.
29. X. Kou, S. Zhang, Z. Yang, C. K. Tsung, G. D. Stucky, L. Sun, J. Wang and C. Yan, *J. Am. Chem. Soc.*, 2007, **129**, 6402-6404.
30. C. K. Tsung, X. Kou, Q. Shi, J. Zhang, M. H. Yeung, J. Wang and G. D. Stucky, *J. Am. Chem. Soc.*, 2006, **128**, 5352-5353.
31. X. Ye, L. Jin, H. Caglayan, J. Chen, G. Xing, C. Zheng, V. Doan-Nguyen, Y. Kang, N. Engheta, C. R. Kagan and C. B. Murray, *ACS Nano*, 2012, **6**, 2804-2817.
32. X. Ye, Y. Gao, J. Chen, D. C. Reifsnyder, C. Zheng and C. B. Murray, *Nano Lett.*, 2013, **13**, 2163-2171.
33. X. Ye, C. Zheng, J. Chen, Y. Gao and C. B. Murray, *Nano Lett.*, 2013, **13**, 765-771.
34. H. Chen, L. Shao, Q. Li and J. Wang, *Chem. Soc. Rev.*, 2013, **42**, 2679-2724.
35. T. Kawano, Y. Niidome, T. Mori, Y. Katayama and T. Niidome, *Bioconj. Chem.*, 2009, **20**, 209-212.
36. B. Van De Broek, F. Frederix, K. Bonroy, H. Jans, K. Jans, G. Borghs and G. Maes, *Nanotechnology*, 2011, **22**.
37. G. Hong, J. T. Robinson, Y. Zhang, S. Diao, A. L. Antaris, Q. Wang and H. Dai, *Angew. Chem. Int. Ed.*, 2012, **51**, 9818-9821.
38. A. Singh, M. Chaudhari and M. Sastry, *Nanotechnology*, 2006, **17**, 2399-2405.
39. S. S. Shankar, A. Rai, B. Ankamwar, A. Singh, A. Ahmad and M. Sastry, *Nat. Mater.*, 2004, **3**, 482-488.
40. R. N. Goyal, A. Aliumar and M. Oyama, *J. Electroanal. Chem.*, 2009, **631**, 58-61.
41. W. L. Huang, C. H. Chen and M. H. Huang, *J. Phys. Chem. C*, 2007, **111**, 2533-2538.
42. J. E. Millstone, S. Park, K. L. Shuford, L. Qin, G. C. Schatz and C. A. Mirkin, *J. Am. Chem. Soc.*, 2005, **127**, 5312-5313.
43. A. Miranda, E. Malheiro, E. Skiba, P. Quaresma, P. A. Carvalho, P. Eaton, B. De Castro, J. A. Shelnett and E. Pereira, *Nanoscale*, 2010, **2**, 2209-2216.
44. T. K. Sau and C. J. Murphy, *J. Am. Chem. Soc.*, 2004, **126**, 8648-8649.
45. S. Xie, N. Lu, Z. Xie, J. Wang, M. J. Kim and Y. Xia, *Angew. Chem. Int. Ed.*, 2012, **51**, 10266-10270.
46. J. Li, Y. Zheng, J. Zeng and Y. Xia, *Chem. Eur. J.*, 2012, **18**, 8150-8156.
47. C. Zhu, J. Zeng, J. Tao, M. C. Johnson, I. Schmidt-Krey, L. Blubaugh, Y. Zhu, Z. Gu and Y. Xia, *J. Am. Chem. Soc.*, 2012, **134**, 15822-15831.
48. R. Marty, G. Baffou, A. Arbouet, C. Girard and R. Quidant, *Opt Express*, 2010, **18**, 3035-3044.
49. S. R. Beeram and F. P. Zamborini, *ACS Nano*, 2010, **4**, 3633-3646.
50. G. Carrot, J. C. Valmalette, C. J. G. Plummer, S. M. Scholz, J. Dutta, H. Hofmann and J. G. Hilborn, *Colloid Polym. Sci.*, 1998, **276**, 853-859.
51. M. S. Bakshi, S. Sachar, G. Kaur, P. Bhandari, M. C. Biesinger, F. Possmayer and N. O. Petersen, *Cryst. Growth Des.*, 2008, **8**, 1713-1719.
52. H. Chen, F. Wang, K. Li, K. C. Woo, J. Wang, Q. Li, L. D. Sun, X. Zhang, H. Q. Lin and C. H. Yan, *ACS Nano*, 2012, **6**, 7162-7171.



We demonstrate that by fine control over experimental parameters triangle Au nanoplates with simultaneously improved purity and edge length can be synthesized by reducing the concentration of CTAB.